Numerical evidence of hyperscaling violation in wetting transitions of the random-bond Ising model in $d = 2$ dimensions

Ezequiel V. Albano and Luciana Luque
Instituto de Física de Líquidos y Sistemas Biológicos (IFLYSIB), CCT-CONICET La Plata, UNLP, Calle 59 Nro. 789, (1900) La Plata, Argentina and Departamento de Física, Facultad de Ciencias Exactas, Universidad Nacional de La Plata, Argentina

Marta L. Trobo
Instituto de Física de Líquidos y Sistemas Biológicos (IFLYSIB), CCT-CONICET La Plata, UNLP, Calle 59 Nro. 789, (1900) La Plata, Argentina and Departamento de Ciencias Básicas, Facultad de Ingeniería, Universidad Nacional de La Plata, Argentina

Kurt Binder
Institute für Physik, Johannes Gutenberg-Universität Mainz, Staudinger Weg 7, D-55099 Mainz, Germany
(Received 3 November 2016; published 1 February 2017)

We performed extensive simulations of the random-bond Ising model confined between walls where competitive surface fields act. By properly taking the thermodynamic limit we unambiguously determined wetting transition points of the system, as extrapolation of localization-delocalization transitions of the interface between domains of different orientation driven by the respective fields. The finite-size scaling theory for wetting with short-range fields [E. V. Albano and K. Binder, Phys. Rev. Lett. **109**, 036101 (2012)] establishes that the average magnetization of the sample, with critical exponent β, is the proper order parameter for the study of wetting. While the hyperscaling relationship given by $\gamma + 2\beta = \nu_\parallel + \nu_\perp$ requires $\beta = 1/2$ ($\gamma = 4$, $\nu_\parallel = 3$, and $\nu_\perp = 2$), the thermodynamic scaling establishes that $\Delta_s = \gamma + \beta$, which in contrast requires $\beta = 0$ ($\Delta_s = 4$), where γ, $\nu_\parallel$, $\nu_\perp$, and Δ_s are the critical exponents of the susceptibility, the correlation lengths parallel and perpendicular to the interface, and the gap exponent, respectively. So, we formulate a finite-size scaling theory for wetting without hyperscaling and perform numerical simulations that provide strong evidence of hyperscaling violation (i.e., $\beta = 0$) and a direct measurement of the susceptibility critical exponent $\gamma/\nu_\perp = 2.0 \pm 0.2$, in agreement with theoretical results for the strong fluctuation regime of wetting transitions with quenched noise.

DOI: 10.1103/PhysRevE.95.022801

I. INTRODUCTION

Understanding the consequences of quenched random disorder in condensed matter has been a challenging problem for decades [1–7] and the associated concepts to deal with free energy landscapes [8] have a remarkable impact on quite different fields such as computer science [9] and biological macromolecules [8]. A generic example is the interface between coexisting phases with opposite orientation of the spontaneous magnetization in an Ising model [10–13]. Already in a "pure" system (i.e., in the absence of any quenched disorder) such an interface in $d \leqslant 3$ dimensions is a critical object, exhibiting long wavelength capillary wave-type fluctuations [14], where the interface gains a lot of entropy by performing local excursions relative to a reference plane (in $d = 3$, at temperatures above the roughening transition) or reference line (in $d = 2$), respectively. On a lateral length scale $L_\parallel$, the typical mean square interfacial width $w^2_{L_\parallel}$ then scales as $\ln L_\parallel$ in $d = 3$, or proportional to $L_\parallel$ in $d = 2$, respectively. The exponent relating $w_{L_\parallel}$ and $L_\parallel$ is called the "wandering exponent" ζ [15,16]

$$w_{L_\parallel} \propto L_\parallel^{\zeta}, \tag{1}$$

and hence $\zeta = 1/2$ in the pure $d = 2$ Ising model.

However, when one has quenched random disorder in the system, this behavior is strongly modified. While the presence of randomly competing signs of the exchange constants J_{ij} between neighboring spins at lattice sites i, j may even destroy the ferromagnetic order (leading to spin glasses [4–9]), and also the case of random magnetic fields $\pm h_r$ destroys order in $d = 2$ [6,17,18], since then $\zeta = 1$ and for large enough L the interfacial tension would turn negative [17]. Here we shall consider only the case of quenched disorder in the magnitude of the exchange constants J_{ij} that are assumed to be ferromagnetic ($J_{ij} > 0$) throughout. Huse *et al.* [19,20] have shown that for the $d = 2$ Ising model with random bonds Eq. (1) holds with

$$\zeta = 2/3, \tag{2}$$

and while in the pure system the prefactor of Eq. (1) vanishes when the temperature $T \to 0$, for the random-bond case Eqs. (1), (2) also hold in the ground state. For the pure system, the straight interface is clearly the single energy minimum, while in the random system the interface is roughened due to the disorder, the (free) energy landscape is rough with many minima, representing competing equivalent rough interface configurations.

This behavior has important implications for wetting phenomena [12,14,21–24]: recall that critical wetting can be viewed as a continuous unbinding transition of the interface from a wall [22], and clearly the interfacial roughness that is enhanced by the bond disorder [Eq. (2)] will affect this behavior distinctly. The critical wetting transition generally shows up as a singularity of the singular part of the surface excess free energy due to the wall from which the interface unbinds, $f_s^{(\mathrm{sing})}(t, H)$. Here, t is the distance from the wetting transition:

e.g., $t = [T_{\rm wet}(h_s) - T]/T_{\rm wet}(h_s)$, if the transition is studied by variation of the temperature, or $t = [h_s - h_w(T)]/h_w(T)$, if the wetting transition of the Ising model is studied by variation of a surface magnetic field h_s acting only on the spins at the free boundary of the (semi-infinite) lattice that represents the "wall." Note that $h_s = h_w(T)$ is just the inverse function of $T = T_{\rm wet}(h_s)$, and H is a bulk magnetic field. The thermodynamic scaling then implies for the singular part of the surface (s) excess free energy

$$f_s^{(\rm sing)}(t,H) = t^{2-\alpha_s}\tilde{F}_s(H|t|^{-\Delta_s}), \tag{3}$$

where α_s and Δ_s are two critical exponents, with $\alpha_s = 0$ and $\Delta_s = 3$ in the "pure" Ising model [12,21,22,25]. From Eq. (3), one readily derives the critical behavior of both the surface excess magnetization m_s and the surface excess susceptibility χ_s [25–28], namely

$$m_s = -(\partial f_s/\partial H)_t \tag{4}$$

and

$$\chi_s = -(\partial^2 f_s/\partial H^2)_t, \tag{5}$$

where in the "pure" Ising model one has ($m_s \propto t^{\beta_s}, \chi_s \propto t^{-\gamma_s}$)

$$\beta_s = 2-\alpha_s-\Delta_s = -1, \quad \gamma_s = -(2-\alpha_s-2\Delta_s) = 4. \tag{6}$$

As for all critical phenomena, the basic quantity to consider is a diverging correlation length, in this case the correlation length $\xi_\parallel$ of fluctuations of the interface height from the wall [$y = h(x)$] in the x direction parallel to the interface [12,15,16,21–26]

$$\xi_\parallel \propto t^{-\nu_\parallel}, \quad \nu_\parallel = 2. \tag{7}$$

While the average distance of the interface from the wall simply is proportional to m_s, the relative excursions of the interface in the y direction relative to the average position are described by the perpendicular correlation length

$$\xi_\perp \propto t^{-\nu_\perp}, \quad \nu_\perp = \zeta\nu_\parallel = 1. \tag{8}$$

The exponent $\nu_\perp = 1$ simply results from using $L_\parallel = \xi_\parallel$ in Eq. (1), which yields then $w_L = \xi_\perp$. Equation (8) also shows that $\nu_\perp = -\beta_s$, i.e., the typical distance of the interface from the wall and the relative excursions are of the same order, and moreover the extension of hyperscaling to interfacial phenomena [21]

$$(d-1)\nu_\parallel = 2 - \alpha_s, \tag{9}$$

holds, with $d = 2$, $\nu_\parallel = 2$, and $\alpha_s = 0$.

In view of the enhancement of interfacial roughness due to random-bond disorder, clarification of the critical wetting behavior in the $d = 2$ random-bond Ising model (RBIM) has found a lot of interest [22,25,29–35]. It has been shown (see [22] for an extensive review) that

$$\nu_\parallel = 3, \quad \alpha_s = 0, \quad \nu_\perp = 2. \tag{10}$$

These results are compatible with $\zeta = \nu_\perp/\nu_\parallel = 2/3$ [Eq. (2)], but violate hyperscaling [Eq. (9)]. However, thermodynamic scaling [Eq. (3)] should still hold, and also the compressibility sum rule [21–25] should hold:

$$\chi_s \propto \xi_\parallel^2, \quad \gamma_s = 6. \tag{11}$$

Recall that unlike for critical phenomena in the bulk ($\chi_b \propto \xi_b^{2-\eta}$) there does not occur an exponent η here [21]. The scaling relationship $\gamma_s = 2\Delta_s - 2 + \alpha_s$ [Eq. (6)] then yields Δ_s, and $\beta_s = 2 - \alpha_s - \Delta_s$ yields β_s, i.e.,

$$\Delta_s = 4, \quad \beta_s = -2. \tag{12}$$

While for critical phenomena in the bulk random-bond disorder is believed to have much less dramatic effects (see, e.g., [3,36]), i.e., the hyperscaling remains valid, and the critical exponents even stay unchanged if the specific heat exponent is negative [37], Eqs. (10)–(12) imply a rather strong change of critical exponents for critical wetting in $d = 2$, as compared to the pure case, and a hyperscaling violation.

The classification of critical wetting transitions shows that wetting for the RBIM belongs to the universality class of the strong fluctuation regime transitions [22,25]. In this regime, very general random walk arguments [16] can be used to express the critical exponents simply in terms of the wandering exponent, e.g.,

$$\nu_\perp = \beta_s = \zeta/(1-\zeta), \quad \nu_\parallel = 1/(1-\zeta),$$
$$\Delta_s = (2-\zeta)/(1-\zeta). \tag{13}$$

The aim of the present paper is to perform a test of some of these predictions by means of Monte Carlo simulations. However, Eqs. (3)–(12) refer to the surface excess free energy of the semi-infinite system with a wall, and Monte Carlo simulations can only be carried out for systems that are finite in all their linear dimensions [38]. Studying a system with two equivalent surfaces a distance L apart [39,40] where a (positive) surface field h_s acts one has the difficulty that for $H = 0$ the system with a negative magnetization in the "bulk" is unstable, the two interfaces unbinding from both walls will meet in the center and annihilate each other. The more natural choice is a situation with antisymmetric walls, where at $y = 0$ a surface field $-|h_s|$ and at $y = L$ a surface field $+|h_s|$ act [41]. This choice of boundary conditions stabilizes a situation with a single interface separating a domain with negative magnetization (below the interface) from a domain with positive magnetization (above the interface). In the nonwet phase the interface is bound to either the lower or upper wall, while in the wet phase the interface freely fluctuates around the center ($y = L/2$) of the system.

When one encounters a situation with two different correlation length exponents in different directions, the standard finite size scaling analysis of simulation data needs modification. For bulk critical phenomena, it has been known since a long time (e.g. [42]) that the generalized aspect ratio $c = L^{\nu_\parallel/\nu_\perp}/M$ should be held constant when both L and M are varied. While it was soon realized [40,43] that anisotropic versions of finite-size scaling theory need to be used for the study of critical wetting, too, this approach was implemented and worked out in detail only recently [27].

Now care is needed when we apply the anisotropic finite-size scaling approach [27] developed to study critical wetting in pure systems to the present situation, since it is known that the bulk finite-size scaling [44] relies on the validity of the hyperscaling relationship for the bulk critical exponents for correlation length ν_b, order parameter β_b, and susceptibility γ_b; namely $d\nu_b = \gamma_b + 2\beta_b$ [45,46]. Complications arise when

hyperscaling [47] does not hold, e.g., for the random field Ising model [6,7] where the problems with finite-size scaling indeed are observed [48]. Thus, in Sec. II, we will recall the main features of the finite-size scaling theory for critical wetting [27] and examine the consequences of the hyperscaling violation [Eq. (9) does not hold for $\nu_\parallel = 3$ and $\alpha_s = 0$] for our finite-size scaling analysis. Section III then defines precisely the model that is studied, Sec. IV gives some details on the simulation method, and Sec. V describes and discusses our numerical results. Finally, our conclusions are stated in Sec. VI.

II. FINITE-SIZE SCALING FOR CRITICAL WETTING WITHOUT HYPERSCALING

The basic assumption of the scaling theory presented in [27] was that the wetting transition in a $L \times M$ geometry with two competing boundary fields $\pm|h_s|$ and keeping $c = L^{\nu_\parallel/\nu_\perp}/M$ fixed can be described in terms of the distribution function $P_{L,M}(m)$ of the total magnetization of the system. This distribution function is clearly bimodal where the interface is bound to either of the walls, but should exhibit a broad peak centered at $m = 0$ in the wet phase. The scaling ansatz that was made is

$$P_{L,M}(m) = \xi_{||}^{\beta/\nu_{||}} \tilde{P}(c, M/\xi_{||}, m\xi_{||}^{\beta/\nu_{||}}). \tag{14}$$

Note that it is assumed that M scales with $\xi_{||}$, the total magnetization m scales as $t^\beta \propto \xi_{||}^{-\beta/\nu_{||}}$, keeping c constant $\xi_\perp$ does not enter, and the prefactor $\xi_{||}^{\beta/\nu_{||}}$ in front of the scaling function $\tilde{P}$ ensures the normalization condition

$$\int_{-1}^{+1} P_{L,M}(m)dm = 1. \tag{15}$$

From Eq. (14) one readily sees that $([...]_{\rm av}$ denotes the averaging over the quenched disorder)

$$[\langle m^k\rangle]_{\rm av} = \xi_{||}^{-k\beta/\nu_{||}} \tilde{m}_k(c, M/\xi_{||}), \quad k = 1,2,\ldots, \tag{16}$$

and hence the total susceptibility becomes

$$k_B T\chi' = LM\left([\langle m^2\rangle]_{\rm av} - [\langle|m|\rangle]_{\rm av}^2\right) = LM\xi_{||}^{-2\beta/\nu_{||}} \tilde{\chi}(c, M/\xi_{||}), \tag{17}$$

where $\tilde{m}_k$ implicitly defined in Eq. (16), and $\tilde{\chi} = \tilde{m}_2 - (\tilde{m}_1)^2$ are scaling functions. Using $L = c^{\nu_\perp/\nu_\parallel} M^{\nu_\perp/\nu_\parallel}$ the susceptibility can be rewritten as $[c^{\nu_\perp/\nu_\parallel}(M/\xi_{||})^{2\beta/\nu_\parallel} \tilde{\chi}(c, M/\xi_{||}) \equiv \tilde{\tilde{\chi}}(c, M/\xi_{||})]$, so that

$$k_B T\chi' = M^{1+\nu_\perp/\nu_{||}-2\beta/\nu_\parallel} \tilde{\tilde{\chi}}(c, M/\xi_{||}). \tag{18}$$

Thus the finite-size scaling prediction for the susceptibility at the wetting transition is $k_B T_w \chi'|_{T_w} \propto M^{1+\nu_\perp/\nu_{||}-2\beta/\nu_\parallel}$. On the other hand, the surface susceptibility according to Eq. (11) should scale as

$$\chi_s = \xi_\parallel^2 \tilde{\chi}_s(M/\xi_{||}), \tag{19}$$

implying a behavior $\chi_s \propto M^2$ at the wetting transition. Since the critical part of χ' can only be due to χ_s, the bulk being not critical at the wetting transition, we conclude

$$k_B T_w \chi'|_{T_w} = L^{-1} k_B T_w \chi_s|_{T_w} \propto M^{2-\nu_\perp/\nu_{||}} = M^{4/3}. \tag{20}$$

This exponent $2 - \nu_\perp/\nu_{||}$ hence should be equal to the above result $1 + \nu_\perp/\nu_{||} - 2\beta/\nu_\parallel$, yielding

$$2\beta = 2\nu_\perp - \nu_{||} = 1, \quad \beta = 1/2, \tag{21}$$

and since we also can write Eq. (20) as

$$k_B T_w \chi'|_{T_w} \propto M^{\gamma/\nu_{||}} = M^{4/3}, \tag{22}$$

hyperscaling [implicit in Eq. (14)] implies $\gamma = 4$, compatible with the hyperscaling relationship for the anisotropic bulk systems

$$\nu_\parallel + \nu_\perp = 5 = \gamma + 2\beta. \tag{23}$$

While the scaling relationship [26]

$$\gamma_s = \gamma + \nu_\perp = 6 \tag{24}$$

is fulfilled, the scaling relationship

$$\beta_s = \beta - \nu_\perp \tag{25}$$

would be compatible with Eq. (12), $\beta_s = -2$, only if $\beta = 0$. The same conclusion emerges when we invoke the standard thermodynamic scaling relationship [47]

$$\Delta_s = \gamma + \beta = 4. \tag{26}$$

Thus there is a contradiction between thermodynamic scaling, which requires

$$\beta = 0, \tag{27}$$

and hyperscaling, which requires $\beta = 1/2$ [20]. The result, Eq. (27), would imply that

$$[\langle|m|\rangle]_{\rm av} = \tilde{m}_1(c, M/\xi_{||}) \tag{28}$$

and

$$[\langle m^2\rangle]_{\rm av} = \tilde{m}_2(c, M/\xi_{||}). \tag{29}$$

As a consequence, one would expect that at the wetting transition (where $\xi_{||} \to \infty$), these moments become independent of the system linear dimension, and hence plotting $[\langle|m|\rangle]_{\rm av}$ and $[\langle m^2\rangle]_{\rm av}$ vs t one should observe for $t = 0$ size-independent crossing points $\tilde{m}_1(c,0)$, $\tilde{m}_2(c,0)$. This property was shown to hold for critical wetting in $d = 2$, where hyperscaling holds. In the present case with quenched disorder, where hyperscaling is violated [Eq. (9) does not hold for $\nu_\parallel = 3, \alpha_s = 0$], thermodynamic scaling (yielding $\beta = 0$) and hyperscaling [yielding $\beta = 1/2$; cf. Eq. (23) with $\nu_\parallel = 3$, $\nu_\perp = 2$, $\gamma = 4$] imply contradictory results.

III. RANDOM-BOND ISING MODEL (RBIM) WITH BOUNDARY FIELDS

We consider the $d = 2$ Ising model on the square lattice, where the exchange constants J_{ij} between nearest neighbors are assumed to be quenched random variables. Thus the Hamiltonian is

$$\mathcal{H}^{\rm RBIM} = -\sum_{\langle ij\rangle} J_{ij} S_i S_j - H \sum_i S_i, \tag{30}$$

where the spin variables (S_i) take on the values -1 and $+1$, $\langle ij\rangle$ means that over nearest-neighbors pairs is summed once, and

the magnetic field H is chosen zero throughout. The quenched random bonds J_{ij} are chosen from a bimodal distribution

$$\mathcal{P}(J_{ij}) = \tfrac{1}{2}[\delta(J_{ij} - J_1) + \delta(J_{ij} - J_2)]. \tag{31}$$

For this model the critical temperature of the bulk ($T_{\rm cb}$) is exactly known [49] given by the equation ($k_B = 1$)

$$\sinh(2J_1/T_{\rm cb})\sinh(2J_2/T_{\rm cb}) = 1.$$

Following Fytas and Theodorakis [36] we choose the special case $J_1 = 4/3, J_2 = 2/3$ (choosing the temperature scale such that $J_1 + J_2 = 2$ [36]) so that $T_{\rm cb} = 2.18802$, $T_{\rm cb}/J_1 = 1.64143$.

In order to study the wetting phenomena, we use a $L\times M$ geometry, with free boundaries at the layer $n = 1$ (where a surface field $-h_s$ acts) and $n = L$ (where a surface field h_s acts), while in the x direction (parallel to these boundary layers) periodic boundary conditions are implied. Thus the total Hamiltonian is

$$\mathcal{H} = \mathcal{H}^{\rm RBIM} + h_s \sum_{i\in n=1} S_i - h_s \sum_{i\in n=L} S_i. \tag{32}$$

IV. DETAILS ON THE MONTE CARLO SIMULATION PROCEDURES

Given the knowledge that it is useful to keep the generalized aspect ratio $c = L^{\nu_\parallel/\nu_\perp}/M = L^{3/2}/M$ constant, and noting that the linear dimensions L, M of the lattice need to be integers, we notice that these requirements are trivially fulfilled if L and M are chosen as second and third powers of an integer. We hence have used the choices $L = 25$, $M = 125$; $L = 36$, $M = 216$; $L = 49$, $M = 343$; and $L = 64$, $M = 512$; so that all our simulations are performed by fixing $c = 1$. Of course, $L \gg 1$ is needed when we study critical phenomena, and thus smaller linear dimensions were not regarded. Since for the present problem cluster algorithms [38] are not useful, and the standard Metropolis algorithm needs to be used [38], larger linear dimensions than the quoted ones were not used either, because the statistical accuracy deteriorates due to critical slowing down severely for too large lattice linear dimensions. Note that already in pure systems fluctuating interfaces are very slow objects; in the present system, free energy barriers due to the rugged free energy landscape that the interface experiences because of the quenched random disorder make the equilibration even more difficult. We used typically 10^7 Monte Carlo steps (MCS) per lattice site to reach equilibrium, and then record averages over 2×10^7 MCS. These numbers clearly are rather modest, but one must remember that an average over about 500–1000 different configurations of the quenched random bonds is mandatory in order to carry out the quenched averaging $[\ldots]_{\rm av}$. It is clear that a substantial larger sample of configurations would be desirable, but this would have required computational resources unavailable to us. The observable that was recorded was just the magnetization per spin

$$m = \frac{1}{LM}\sum_{i=1}^{LM} S_i \tag{33}$$

in the system, from which the moments $[\langle|m|\rangle]_{\rm av}$ and $[\langle m^2\rangle]_{\rm av}$ considered in Sec. II were constructed, as well as the reduced

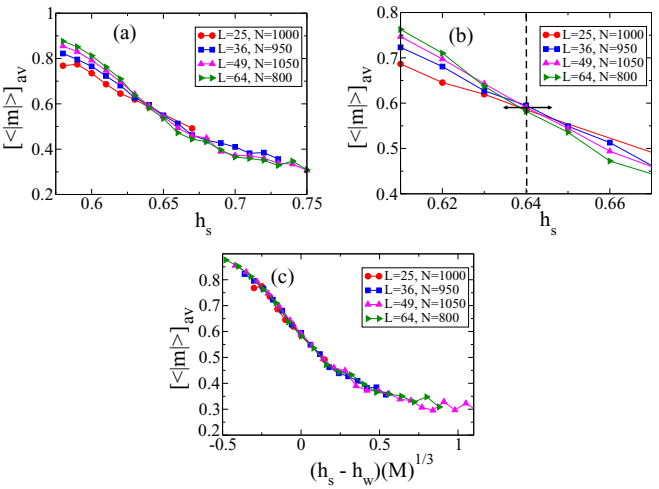

FIG. 1. (a) Plots of the average absolute value of the magnetization $[\langle|m|\rangle]_{\rm av}$ vs h_s. Data corresponding to temperature $T = 1.75$ are shown. The size of the samples and the number of averages over different configurations (N) are indicated. All sample sizes have the same generalized aspect ratio $c = L^{3/2}/M = 1$. (b) Zoom of the data shown in (a) in order to show the common intersection point of the data. The vertical (dashed) line shows the intersection point of the magnetization measured for samples of different size, while the horizontal (solid) line gives an estimation of the error in the evaluation of the critical point. (c) Scaling plot of the absolute value of the magnetization vs $(h_s - h_w)\times M^{1/3}$, showing the data collapse obtained by taking $\beta = 0$, and $h_w = 0.64$. More details in the text.

fourth order cumulant

$$U = 1 - \frac{[\langle m^4\rangle]_{\rm av}}{3[\langle m^2\rangle]^2_{\rm av}}. \tag{34}$$

V. SIMULATION RESULTS

Given the knowledge that (for our choice of units) $T_{\rm cb} = 2.18802$, we hence studied two temperatures $T = 1.50$ and $T = 1.75$, varying the strength of the magnitude of the boundary fields $|h_s|$. Of course, we must not work at rather low temperatures, since then the free energy barriers constraining the interfacial fluctuations slow down the dynamics too much; on the other hand, we must not work close to $T_{\rm cb}$ either, to avoid crossover towards bulk criticality. Thus, after a careful evaluation, we conclude that the choices $T = 1.50$ and $T = 1.75$ are acceptable compromises between these two conflicting requirements. We describe the results for $T = 1.75$ first.

Figures 1 and 2 show our data for $[\langle|m|\rangle]_{\rm av}$, and $[\langle m^2\rangle]_{\rm av}$, plotting them *versus* h_s [part (a)] and $(h_s - h_w)M^{1/3}$ [part (c)]. The estimate of the critical field $h_w(T) \simeq 0.640 \pm 0.006$ was extracted from the common intersection point of $[\langle|m|\rangle]_{\rm av}$ and $[\langle m^2\rangle]_{\rm av}$ [see amplified plots in part (b) of Figs. 1,2]. The fact that such common intersection points occur are a clear evidence that $\beta = 0$ [i.e., Eq. (27) rather than Eq. (21) is valid]. The common intersection point close to $h_s = 0.64$ is also observed for the cumulant [Fig. 3(a)]; however, the accuracy in the determination of the critical point decreases due to both the smooth dependence of U on h_s, and the lack of appropriate statistics in our data.

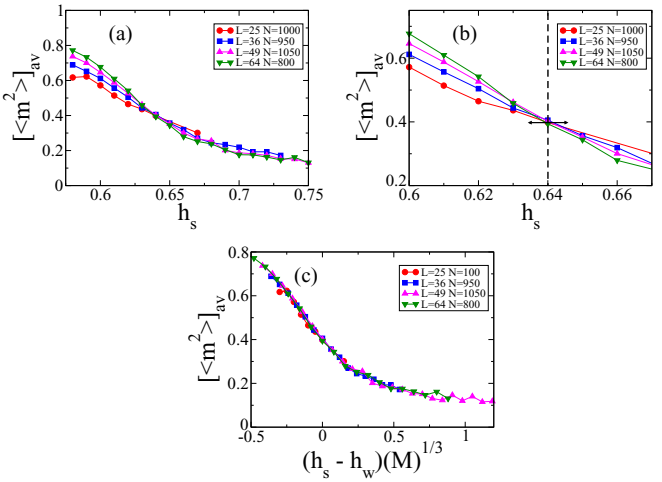

FIG. 2. (a) Plots of the average square magnetization $[\langle m^2\rangle]_{\rm av}$ vs h_s. Data corresponding to temperature $T = 1.75$ are shown. The size of the samples and the number of averages over different configurations (N) are indicated. All sample sizes have the same generalized aspect ratio $c = L^{3/2}/M = 1$. (b) Zoom of the data shown in (a) in order to show the common intersection point of the data. The vertical (dashed) line shows the intersection point of the magnetization measured for samples of different size, while the horizontal (solid) line gives an estimation of the error in the evaluation of the critical point. (c) Scaling plot of the square magnetization vs $(h_s - h_w) \times M^{1/3}$, showing the data collapse obtained by taking $\beta = 0$, and $h_w = 0.64$. More details in the text.

The scaling plots, using the variable $(h_s - h_w) \times M^{1/3}$, are of reasonable quality, Figs. 1(c), 2(c), and 3(b), given the moderate statistical accuracy of our data, and hence imply that our data are indeed compatible with a scaling variable $M/\xi_{||} \propto M|h_s - h_w|^3$, as expected. Thus, although hyperscaling fails, a restricted form of finite-size scaling seems to remain valid.

Figures 4 and 5 focus on the susceptibility $T\chi' = LM([\langle m^2\rangle]_{\rm av} - [\langle |m|\rangle]^2_{\rm av})$. Given that at the wetting transition

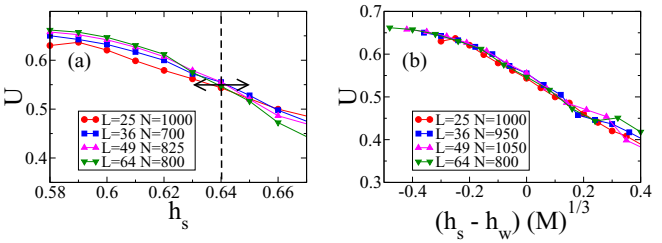

FIG. 3. Cumulant U plotted vs h_s showing data corresponding to temperature $T = 1.75$. The size of the samples and the number of averages over different configurations (N) are indicated. All sample sizes have the same generalized aspect ratio $c = L^{3/2}/M = 1$. (a) Zoom of the data of the plots of the cumulant U vs h_s, in order to show the common intersection point of the data. The vertical (dashed) line shows the intersection point of the cumulant measured for samples of different size, while the horizontal (solid) line gives an estimation of the error in the evaluation of the critical point. (b) Scaling plot of the cumulant vs $(h_s - h_w) \times M^{1/3}$, showing the data collapse obtained by assuming $h_w = 0.64$. More details in the text.

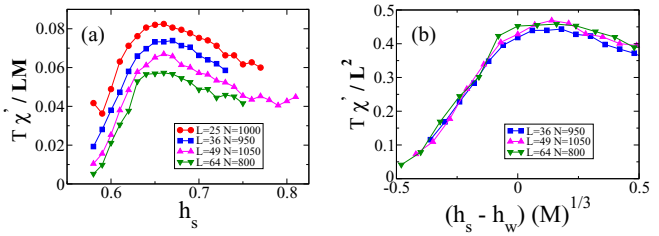

FIG. 4. (a) Plots of the susceptibility $T\chi'/LM$ vs h_s. Data corresponding to temperature $T = 1.75$ are shown. The size of the samples and the number of averages over different configurations (N) are indicated. All sample sizes have the same generalized aspect ratio $c = L^{3/2}/M = 1$. (b) Scaling plot of the susceptibility $T\chi'/L^2$ vs $(h_s - h_w) \times M^{1/3}$ with $h_w = 0.64$.

both $[\langle |m|\rangle]_{\rm av}$ and $[\langle m^2\rangle]_{\rm av}$ are finite constants of order unity (the ordinate values of the intersection points in Figs. 1, 2) one might expect that $T\chi'/LM$ are also finite constants of order unity at the intersection points as well, independent of the size. However, Fig. 4(a) demonstrates that this is not the case since $T\chi'/LM$ is not of order unity, but rather very small, and decreases systematically with increasing size. In fact, if $\beta = 0$ and $\tilde{\chi}'(c,0)$ in Eq. (17) exists, the conclusion $T\chi'/LM =$ const for $h_s = h_w(T)$ is inevitable. Also, if Eq. (14) holds, then Eq. (18) with $\tilde{\chi}'(c,0) =$ const would yield for $\beta = 0$

$$k_B T\chi'|_{h_w} \propto M^{1+\nu_\perp/\nu_{||}} = M^{5/3} \propto L^{5/2}, \tag{35}$$

while the numerical evidence [Figs. 4(b) and 5] compellingly shows

$$k_B T\chi'|_{h_w} \propto M^{4/3} \propto L^2. \tag{36}$$

This result clearly is compatible with Eqs. (19), (20), and we conclude again that $\gamma = 4$, $\beta = 0$, and the restricted form of finite-size scaling [Eq. (14)] still is valid, with the scaling function $\tilde{P}(c, M/\xi_{||}, m\xi_{||}^{\beta/\nu_{||}})$ that has the property that the scaling function $\tilde{\chi}'(c, M/\xi_{||})$ vanish, and the leading correction term to Eqs. (17), (18), survives and replaces the proper behavior [Eqs. (19), (20)]. Note that in the limit $M/\xi_\parallel \to 0$ the factor $\xi_\parallel^{-2\beta/\nu_\parallel}$ in Eq. (17) should cancel out. If we hence would assume $\tilde{\chi}(c, M/\xi_\parallel \to 0) = \text{const}\xi_\parallel^{2\beta/\nu_\parallel} M^{-2\beta/\nu_\parallel}$, we would obtain $k_B T\chi' = \text{const} LM^{1-2\beta/\nu_\parallel} = \text{const} L^{1+\nu_\parallel/\nu_\perp - 2\beta/\nu_\perp} c^{-(1-2\beta/\nu_\perp)}$,

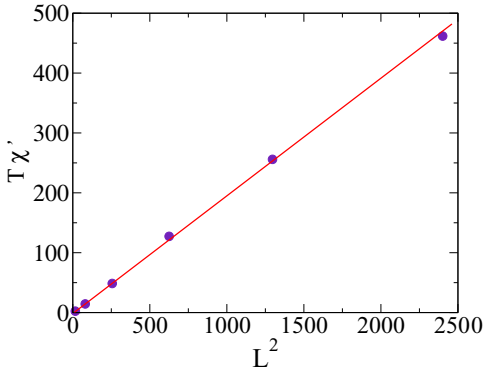

FIG. 5. Plot of $T\chi'$ vs $L^{\gamma/\nu_\perp} = L^2$ as obtained at $T = 1.75$ by using data measured at the wetting transition. The straight line has been drawn in order to guide the eye. More details in the text.

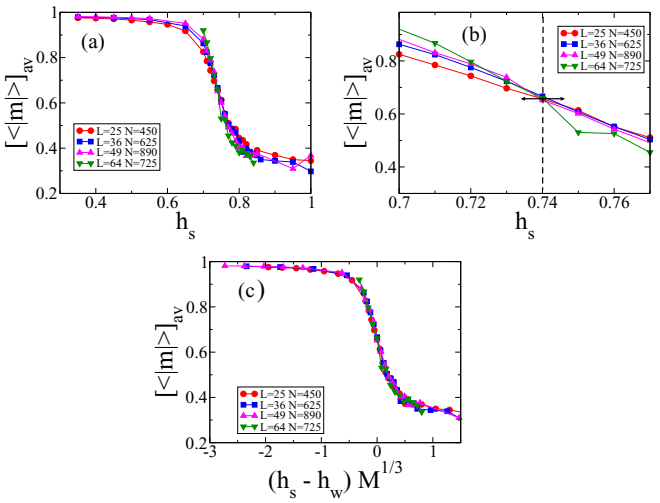

FIG. 6. (a) Plots of the average absolute value of the magnetization $[\langle|m|\rangle]_{\rm av}$ vs h_s. Data corresponding to temperature $T = 1.50$. The size of the samples and the number of averages over different configurations (N) are indicated. All sample sizes have the same generalized aspect ratio $c = L^{3/2}/M = 1$. (b) Zoom of the data shown in (a) in order to show the common intersection point of the data. The vertical (dashed) line shows the intersection point of the magnetization measured for samples of different size, while the horizontal (solid) lines give an estimation of the error in the evaluation of the critical point. (c) Scaling plot of the absolute value of the magnetization vs $(h_s - h_w) \times M^{1/3}$, showing the data collapse obtained by taking $\beta = 0$, and $h_w = 0.74$. More details in the text.

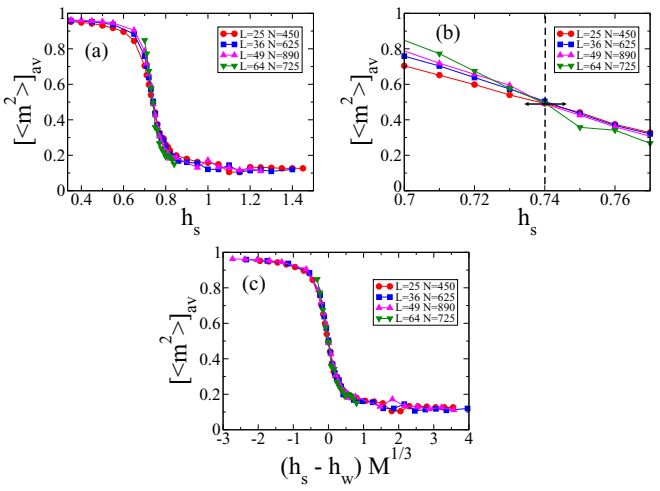

FIG. 7. (a) Plots of the average square magnetization $[\langle m^2\rangle]_{\rm av}$ vs h_s. Data corresponding to temperature $T = 1.50$ are shown. The size of the samples and the number of averages over different configurations (N) are indicated. All sample sizes have the same generalized aspect ratio $c = L^{3/2}/M = 1$. (b) Zoom of the data shown in (a) in order to show the common intersection point of the data. The vertical (dashed) line shows the intersection point of the magnetization measured for samples of different size, while the horizontal (solid) lines give an estimation of the error in the evaluation of the critical point. (c) Scaling plot of the square magnetization vs $(h_s - h_w) \times M^{1/3}$, showing the data collapse obtained by taking $\beta = 0$, and $h_w = 0.74$. More details in the text.

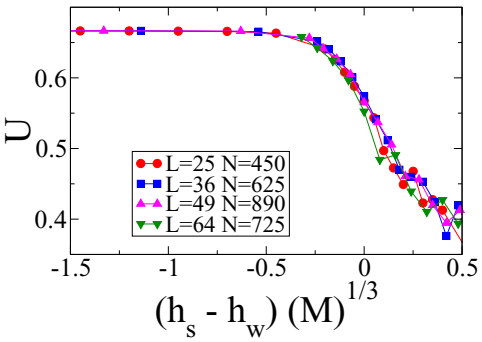

FIG. 8. Scaling plot of the cumulant vs $(h_s - h_w) \times M^{1/3}$, showing the data collapse obtained by assuming $h_w = 0.74$. Data corresponding to temperature $T = 1.50$ are shown. The size of the samples and the number of averages over different configurations (N) are indicated. All sample sizes have the same generalized aspect ratio $c = L^{3/2}/M = 1$. More details in the text.

i.e., $k_B T \chi' \propto L^{5/2}$ if $\beta = 0$. A contradiction with the correct result $k_B T \chi' \propto L^2$ at the transition is avoided, however, when the above constant actually is zero, i.e., when the scaling functions $\tilde{m}_1(c, M/\xi_\parallel)$ and $\tilde{m}_2(c, M/\xi_\parallel)$ and have the particular limiting behavior

$$\tilde{m}_2(c, M/\xi_\parallel \to 0) = (\tilde{m}_1(c, M/\xi_\parallel \to 0))^2. \qquad (37)$$

As we have demonstrated in Figs. 1(c) and 2(c), there is numerical evidence that the first and second moment of the magnetization distribution indeed exhibit the postulated scaling with $M/\xi_\parallel$, or equivalently with $(h - h_s)M^{1/3}$.

The second temperature $T = 1.50$ (Figs. 6–10) corroborates these findings, though the accuracy is clearly less. Here the transition occurs at a somewhat larger field [$h_w(T) \simeq 0.740 \pm 0.07$; see Figs. 6(b), 7(b)] and the variation with h_s is somewhat steeper, but a reasonable quality of scaling against the variable $(h_s - h_w) \times M^{1/3}$ is still observed [Figs. 6(c), 7(c), and 8]. Also, the relation $\chi'|_{h_w} \propto L^2$ is again nicely confirmed (Fig. 10). Notice that the fluctuations of $T\chi'/LM$ in the unscaled data [Fig. 9(a)] are somewhat more pronounced than the corresponding plot for $T = 1.75$ [Fig. 4(a)]. However, Fig. 9(b) indicates that the scaling $T\chi'/L^2$ versus

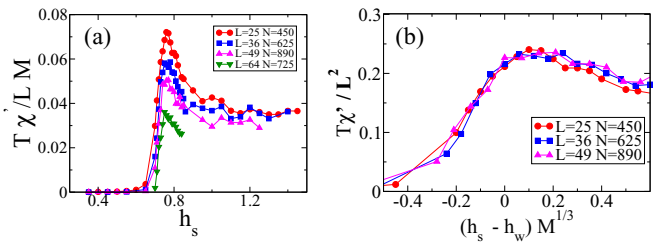

FIG. 9. (a) Plots of the susceptibility $T\chi'/LM$ vs h_s. Data corresponding to temperature $T = 1.50$ are shown. The size of the samples and the number of averages over different configurations (N) are indicated. All sample sizes have the same generalized aspect ratio $c = L^{3/2}/M = 1$. (b) Scaling plot of the $T\chi'/L^2$ vs $(h_s - h_w) \times M^{1/3}$, and $h_w = 0.74$.

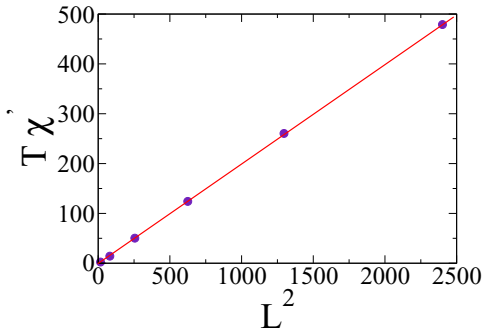

FIG. 10. Plot of $T\chi'$ vs $L^{\gamma/\nu_\perp} = L^2$ as obtained at $T = 1.50$ by using data measured at the wetting transition. The straight line has been drawn in order to guide the eye. More details in the text.

$(h_s - h_w) \times M^{1/3}$ holds reasonably well, but data corresponding to the largest lattice ($L = 64$, $M = 512$) have been disregarded since they are markedly below the scaling function; presumably this is an indication that critical slowing down may not be neglected. Summing up, we conclude that the data for $T = 1.50$ as a whole confirms the conclusions on the nature of the critical phenomena at the wetting transition, as drawn above.

VI. CONCLUSIONS

Understanding the effects of quenched random disorder on the statistical mechanics of phase transitions and in particular critical phenomena has been a longstanding challenge. A particularly interesting case is critical wetting in $d = 2$ dimensions in the presence of random impurities, which create a disorder of the random-bond type in the framework of an Ising model description. Physically, this system can be realized if a monolayer of some adsorbate can condense on a substrate surface, where wetting at a surface step may occur [40,41] and a quenched disorder is present due to some point defects on the substrate (e.g., due to irreversibly chemisorbed atoms or molecules of some other material). But apart from this possibility of an experimental realization, the interest of this problem is mainly due to the fact that the critical exponents for this interface unbinding transition are believed to be known exactly [22,26,29–35], and violate the hyperscaling relationship (for $d = 2$ critical wetting) $\nu_{||} = 2 - \alpha_s$, since $\nu_{||} = 3$ and $\alpha_s = 0$ here. In contrast, for critical wetting in $d = 2$ dimensions without randomly quenched disorder this relationship is known to be valid ($\nu_{||} = 2$ and $\alpha_s = 0$) [12,21].

This violation of hyperscaling has special consequences for the description of critical wetting in the finite-size scaling limit. This limit considers the thermodynamic limit (linear dimension M of the boundary from which the interface unbinds tending to infinity, $M \to \infty$) in a thin film geometry keeping the generalized aspect ratio c constant (linear dimension L of the film in the direction perpendicular to the boundary being chosen such that $c = L^{\nu_{||}/\nu_\perp}/M$, $\nu_\perp$ being the correlation length exponent associated with the correlation length $\xi_\perp$ in the direction perpendicular to the interface). In an Ising model description, the two boundary fields of opposite sign ($\pm|h_s|$) act at the opposite boundaries of the thin film (or strip, respectively). Below the wetting critical temperature [$T_w^c(h_s)$] the interface is bound to one of the boundaries, so there is nonzero magnetization (per spin) in the strip;; the distribution $P_{L,M}(m)$ is peaked [27] near $\pm\langle|m|\rangle$. However, for temperatures above $T_w^c(h_s)$, but below the bulk critical temperature, there exists an interface, between two domains of opposite sign of the magnetization, unbound from the boundaries, freely fluctuating in the middle of the strip, i.e., $P_{L,M}(m)$ is peaked at $m = 0$. For the wetting transition, the magnetization $\langle|m|\rangle$ and its "susceptibility" χ' [defined in terms of the fluctuation relation $k_B T\chi' = LM(\langle m^2\rangle - \langle|m|\rangle^2)$] there exhibit critical singularities, $\langle|m|\rangle \propto (1 - T/T_w^c(h_s))^\beta$, $\chi' \propto (1 - T/T_w^c(h_s))^{-\gamma}$, and for a system without randomly quenched disorder, an anisotropic version of hyperscaling holds [27], $2\beta + \gamma = \nu_{||} + \nu_\perp$ [with $\beta = 0$, $\gamma = 3$, $\nu_{||} = 2$, and $\nu_\perp = 1$; Eq. (22)]. These exponents also satisfy the standard thermodynamic scaling relation $\beta + \gamma = \Delta_s$, with the "gap exponent" Δ_s that appears also in the surface excess free energy $f_s^{(\mathrm{sing})}(t,H) = t^{2-\alpha_s}\tilde{F}_s(H|t|^{-\Delta_s})$, where $t = 1 - T/T_w^c(h_s)$ and H is the bulk field [Eq. (3)]. While this thermodynamic scaling relation is also true in the case where quenched disorder is present [25], with $\Delta_s = 4$, $\gamma = 4$, $\beta = 0$, these exponents clearly are incompatible with the above hyperscaling relation, Eq. (22), which would require $\beta = 1/2$ when $\nu_{||} = 3$, $\nu_\perp = 2$, and $\gamma = 4$. In fact, an exponent $\beta = 0$ in Eq. (17), which relies implicitly on hyperscaling, is only compatible with $\gamma = 4$ ($\chi' \propto M^{\gamma/\nu_{||}} = M^{4/3} = L^2$), if the quantity $\tilde{\tilde{\chi}}(c,0)$ introduced in Eq. (17) vanishes. It hence is required that the average distribution $P_{L,M}(m)$ for $T < T_w^c(h_s)$ has two peaks whose widths asymptotically vanish relative to their position.

Both cases of critical wetting in $d = 2$, pure systems with a wandering exponent $\zeta = 1/2$ and the RBIM with $\zeta = 2/3$, are interesting examples of wetting transitions in the strong fluctuation universality class, and the numerical verification of the rich theoretical predictions [16,19,20,22,25,29–35] available for this class are of interest.

In the present work, we have studied this very unusual scenario of a critical wetting transition by extensive Monte Carlo simulations. The task is computationally very demanding, since for a decent accuracy both long runs are required (since the interfacial fluctuations are very slow if both L and M are large) and the quenched average $[\ldots]_{\mathrm{av}}$ over the distribution of the random-bond configuration requires a sample of the order of $N = 10^3$ configurations (Figs. 1–10). The evidence for $\beta = 0$, however, is very straightforwardly obtained from the fact that $[\langle|m|\rangle]_{\mathrm{av}}$ and $[\langle m^2\rangle]_{\mathrm{av}}$ plotted versus h_s show common intersection points (Figs. 1, 2 and 6, 7), that are mutually consistent with each other. At both temperatures that were studied a finite-size scaling compatible with $(h_s - h_w(T)) \times M^{1/3}$ is obeyed, as expected when $\nu_{||} = 3$. The normalized susceptibility $T\chi'/LM$ is found to decrease systematically with increasing linear dimensions [Figs. 4(a), and 9(a)], and scales when plotted as $T\chi'/L^2$ (and hence does not scale when $M = L^{3/2}$ is invoked), Figs. 4(b), and 9(b). Indeed at the transition the result $LM\chi' \propto L^2$ is compellingly verified (Figs. 5 and 10). The fact that the observed exponents are the same at both temperatures $T = 1.75$ and $T = 1.5$ that were studied is expected from the principle of universality, of course.

In conclusion, we think that our study demonstrates that the effects of quenched random disorder in the (ferromagnetic)

bonds of an Ising model on the critical wetting transition are correctly described by the available theory.

ACKNOWLEDGMENTS

We are greatly indebted to Professor M. Kardar for drawing our attention to the available theoretical predictions and for suggesting that a Monte Carlo study of this problem would be of interest. One of us (E.V.A.) acknowledges the support of the Alexander von Humboldt Foundation and the Deutsche Forschungsgemeinschaft (DFG), Grant No. SFB TR 146, for partial support of his stay at the Institut für Physik of the Johannes Gutenberg Universität Mainz (Germany). Also, E.V.A., L.L., and M.L.T. acknowledge the financial support of CONICET and UNLP (Argentina).

[1] R. Brout, Phys. Rev. **115**, 824 (1959).
[2] J. M. Ziman, *Models of Disorder: The Theoretical Physics of Homogeneously Disordered Systems* (Cambridge University Press, Cambridge, UK, 1979).
[3] R. B. Stinchombe, in *Phase Transitions and Critical Phenomena*, edited by C. Domb and J. L. Lebowitz (Academic Press, London, 1983), Vol. VII, p. 151.
[4] K. Binder and A. P. Young, Rev. Mod. Phys. **58**, 801 (1986).
[5] M. Mézard, G. Parisi, and M. Virasoro, *Spin Glass Theory and Beyond* (World Scientific, Singapore, 1987).
[6] *Spin Glasses and Random Fields*, edited by A. P. Young (World Scientific, Singapore, 1997).
[7] K. Binder and W. Kob, *Glassy Materials and Disordered Solids: An Introduction to their Statistical Mechanics* (World Scientific, Singapore, 2011).
[8] *Rugged Free Energy Landscapes: Common Computational Approaches to Spin Glasses, Structural Glasses, and Biological Macromolecules*, edited by W. Janke (Springer, Berlin, 2008).
[9] M. Mézard and A. Montanari, *Information, Physics, and Computation* (Oxford University Press, Oxford, 2009).
[10] B. Widom, in *Phase Transitions and Critical Phenomena*, edited by C. Domb and M. S Green (Academic Press, London, 1972), Vol. II, p. 79.
[11] D. Jasnow, Rep. Prog. Phys. **47**, 1059 (1984).
[12] D. B. Abraham, in *Phase Transitions and Critical Phenomena*, edited by C. Domb and J. L. Lebowitz (Academic Press, London, 1986), Vol. X, p. 1.
[13] K. Binder, B. Block, S. K. Das, and P. Virnau, J. Stat. Phys. **144**, 690 (2011).
[14] J. S. Rowlinson and B. Widom, *Molecular Theory of Capillarity* (Clarendon Press, Oxford, 1982).
[15] M. E. Fisher, J. Stat. Phys. **34**, 667 (1984).
[16] M. E. Fisher, J. Chem. Soc., Faraday Trans. **82**, 1589 (1986).
[17] K. Binder, Z. Phys. B **50**, 343 (1983).
[18] T. Nattermann, in *Spin Glasses and Random Fields*, edited by A. P. Young (World Scientific, Singapore, 1998), p. 277.
[19] D. A. Huse and Ch. L. Henley, Phys. Rev. Lett. **54**, 2708 (1985).
[20] D. A. Huse, Ch. L. Henley, and D. S. Fisher, Phys. Rev. Lett. **55**, 2924 (1985).
[21] S. Dietrich, in *Phase Transitions and Critical Phenomena*, edited by C. Domb and J. L. Lebowitz (Academic Press, New York, 1988), Vol. XII, p. 1.
[22] G. Forgacs, R. Lipowsky, and T. M. Nieuwenhuizen, in *Phase Transitions and Critical Phenomena*, edited by C. Domb and J. L. Lebowitz (Academic Press, New York, 1991), Vol. XIV, p. 136.
[23] D. Bonn and D. Ross, Rep. Prog. Phys. **64**, 1085 (2001).
[24] D. Bonn, J. Eggers, J. Indekeu, J. Meunier, and E. Rolley, Rev. Mod. Phys. **81**, 739 (2009).
[25] A. O. Parry, M. J. Greenall, and A. J. Wood, J. Phys.: Condens. Matter **14**, 1169 (2002).
[26] K. Binder, in *Phase Transitions and Critical Phenomena*, edited by C. Domb and J. L. Lebowitz (Academic Press, London, 1983), Vol. VIII, p. 1.
[27] E. V. Albano and K. Binder, Phys. Rev. E **85**, 061601 (2012); Phys. Rev. Lett. **109**, 036101 (2012).
[28] To avoid confusion we note that Parry *et al.* [25] define β_s with the opposite sign. However, we prefer to use the traditional definition [26] that emphasizes the analogy with scaling laws in the bulk.
[29] M. Kardar, Phys. Rev. Lett. **55**, 2235 (1985).
[30] R. Lipowsky and M. E. Fisher, Phys. Rev. Lett. **56**, 472 (1986).
[31] R. Lipowsky and M. E. Fisher, Phys. Rev. B **36**, 2126 (1987).
[32] M. Kardar, Nucl. Phys. B **290**, 582 (1987).
[33] R. Lipowsky, Phys. Scr., T **29**, 259 (1989).
[34] M. Huang, M. E. Fisher, and R. Lipowsky, Phys. Rev. B **39**, 2632 (1989).
[35] J. Wuttke and R. Lipowsky, Phys. Rev. B **44**, 13042 (1991).
[36] N. G. Fytas and P. E. Theodorakis, Eur. J. Phys. B **86**, 30 (2013).
[37] A. B. Harris, J. Phys. C **7**, 1671 (1974).
[38] D. P. Landau and K. Binder, *A Guide to Monte Carlo Simulation in Statistical Physics*, 4th ed. (Cambridge University Press, Cambridge, UK, 2015).
[39] K. Binder and D. P. Landau, Phys. Rev. B **37**, 1745 (1988).
[40] E. V. Albano, K. Binder, D. W. Heermann, and W. Paul, J. Stat. Phys. **61**, 161 (1990).
[41] E. V. Albano, K. Binder, D. W. Heermann, and W. Paul, Surf. Sci. **223**, 151 (1989).
[42] K. Binder and J. S. Wang, J. Stat. Phys. **55**, 87 (1989).
[43] A. O. Parry and R. Evans, Physica A **181**, 250 (1992).
[44] *Finite-size Scaling and Numerical Simulation of Statistical Systems*, edited by V. P. Privman (World Scientific, Singapore, 1990).
[45] K. Binder, Z. Phys. B **43**, 119 (1981).
[46] E. Brézin, J. Phys. (Paris) **43**, 15 (1982).
[47] M. E. Fisher, Rev. Mod. Phys. **46**, 597 (1974).
[48] R. L. C. Vink, T. Fischer, and K. Binder, Phys. Rev. E **82**, 051134 (2010).
[49] R. Fish, J. Stat. Phys. **18**, 111 (1978).